Opportunities to Intercalibrate Radiometric Sensors from International Space Station

C. M. ROITHMAYR, C. LUKASHIN, P. W. SPETH, D. F. YOUNG, AND B. A. WIELICKI

NASA Langley Research Center, Hampton, Virginia

K. J. THOME

NASA Goddard Space Flight Center, Greenbelt, Maryland

G. KOPP

Laboratory for Atmospheric and Space Physics, University of Colorado Boulder, Boulder, Colorado

(Manuscript received 31 July 2013, in final form 2 December 2013)

ABSTRACT

Highly accurate measurements of Earth's thermal infrared and reflected solar radiation are required for detecting and predicting long-term climate change. Consideration is given to the concept of using the International Space Station to test instruments and techniques that would eventually be used on a dedicated mission, such as the Climate Absolute Radiance and Refractivity Observatory (CLARREO). In particular, a quantitative investigation is performed to determine whether it is possible to use measurements obtained with a highly accurate (0.3%, with 95% confidence) reflected solar radiation spectrometer to calibrate similar, less accurate instruments in other low Earth orbits. Estimates of numbers of samples useful for intercalibration are made with the aid of yearlong simulations of orbital motion. Results of this study support the conclusion that the International Space Station orbit is ideally suited for the purpose of intercalibration between spaceborne sensors.

1. Introduction

It is essential that we understand the nature of the changes taking place in Earth's climate, correctly attribute the changes to natural variability or anthropogenic effects, make reliable long-term forecasts for the magnitude of those changes, and act accordingly. We must have high confidence in our predictions of climate because our response may entail enormous societal and economic costs.

Earth's thermal infrared and reflected solar radiation are among the quantities that must be measured accurately on a global scale over long time spans in order to gain the necessary understanding and ability to predict climate change. Current methods of measuring these two variables from spacecraft are not sufficiently accurate; an order of magnitude improvement is required in the case of reflected solar radiation (Wielicki et al. 2013). Two proposed complementary missions address the need for greater accuracy by employing instruments with onboard calibration that permits traceability to international metrological standards. The first of these, Climate Absolute Radiance and Refractivity Observatory (CLARREO) (Wielicki et al. 2013), is one of the four top-priority missions recommended in the 2007 decadal survey report by the National Research Council (2007). The second, Traceable Radiometry Underpinning Terrestrial- and Helio- Studies (TRUTHS) (Fox et al. 2003, 2011), is proposed by the U.K. National Physical Laboratory. The highly accurate measurements obtained from such missions are important not only for their intrinsic value as climate benchmarks but also for their usefulness in calibrating less accurate radiometric instruments aboard other spacecraft. Through a process known as reference intercalibration, the accuracy of other instruments can be improved significantly, thereby enhancing the performance of an entire climate observation *system*. Intercalibration requires detailed data matching—that is, measurements from two spacecraft must be taken along similar lines of sight, and within a few minutes of each other. Similar techniques are currently used for intercalibration of orbiting satellite sensors as part of the

Corresponding author address: Constantine Lukashin, NASA Langley Research Center, MS 420, Hampton, VA 23681.
E-mail: constantine.lukashin-1@nasa.gov

DOI: 10.1175/JTECH-D-13-00163.1

© 2014 American Meteorological Society

Global Space-Based Inter-Calibration System (GSICS), an international effort to improve the consistency of satellite intercalibration. The current system, however, lacks an orbiting high-accuracy International System of Units (SI)-traceable reference radiometer comparable to CLARREO. GSICS has indicated measurements from such an instrument form a critical element in anchoring satellite observations, especially for climate applications (Goldberg et al. 2011).

Despite a well-established need, recognition of the important advantages, and extensive preparatory research conducted thus far, there are currently no firm plans for dedicated satellite missions such as CLARREO and TRUTHS. Considerable thought is, however, being given to placing CLARREO instruments on alternative orbiting platforms in order to test equipment and techniques and make it possible to obtain the benefits of highly accurate measurements before dedicated spacecraft can be put into service. In this regard the International Space Station (ISS) appears to be an attractive platform for several reasons.

First, there is at present significant interest in conducting studies of global climate change from the ISS, as evidenced by the Announcement of Opportunity (ESA 2011) issued by the European Space Agency in 2011, and a large number of proposals received in response to a preceding call for ideas in 2009. The National Aeronautics and Space Administration (NASA) Science Mission Directorate provided a similar avenue in 2011 with the Earth Venture–2 Announcement of Opportunity (NASA 2011). Second, in connection with measurements of thermal infrared and reflected solar radiation specifically, an advantageous relationship exists between the ISS orbit and the sun-synchronous orbits in which radiometric sensors are often placed. The orbit plane of ISS precesses westward with respect to an inertial frame of reference, completing a full revolution in about 72 days. The period of eastward precession for the orbit plane of a sun-synchronous spacecraft is one year. Consequently, alignment of the ascending nodes of the two orbits goes through a cycle whose period is 60 days; thus, measurements can be compared for viewing geometry conditions that recur every 60 days. Furthermore, the ISS orbital altitude is approximately 400 km less than that of key sun-synchronous satellites, resulting in relatively gradual changes in direction of the line of sight between spacecraft. Third, the long projected service life of ISS, together with the presence of a human crew and robotic equipment, makes it possible to consider operational options that will not be available at other spacecraft. In particular, failed equipment can be serviced and repaired, the instrument can be replaced every few years on a regular basis, and the instrument can be returned to Earth for postflight evaluations and possible refurbishment. All of the aforementioned considerations indicate ISS can be a useful stepping-stone on the way to dedicated missions such as CLARREO and TRUTHS.

As a precursor to a free-flying CLARREO mission, two top-of-atmosphere instruments could be placed on ISS: a thermal infrared upward radiation spectrometer and a reflected solar radiation spectrometer. These instruments would serve the international community by intercalibrating other Earth-observing instruments, including, but not limited to, Advanced Baseline Imager (ABI), Advanced Geostationary Radiation Imager (AGRI), Advanced Himawari Imager (AHI), Atmospheric Sounding Interferometer (ASI), Advanced Very High Resolution Radiometer (AVHRR), Clouds and the Earth's Radiant Energy System (CERES), Cross-Track Infrared Sounder (CrIS), Enhanced Thematic Mapper Plus (ETM+), Flexible Combined Imager (FCI), Geostationary Interferometric Infrared Sounder (GIIRS), Global Ozone Monitoring Experiment-2 (GOME-2), High Resolution Infrared Radiation Sounder (HIRS), Infrared Atmospheric Sounding Interferometer (IASI), Infrared Atmospheric Sounder (IRAS), Infrared Sounder (IRS), Medium Resolution Spectral Imager-2 (MERSI-2), Moderate Resolution Imaging Spectroradiometer (MODIS), Ocean and Land Color Imager (OLCI), Spinning Enhanced Visible Infrared Imager (SEVIRI), Second-Generation Global Imager (SGLI), Sea and Land Surface Temperature Radiometer (SLSTR), Visible Infrared Imager Radiometer Suite (VIIRS), and Visible and Infrared Radiometer (VIRR).

Several of the foregoing instruments are in geosynchronous Earth orbit (GEO). In some respects, it is more straightforward to intercalibrate these instruments than sensors in low Earth orbit (LEO). Three or four intercalibration opportunities arise each day, and a single opportunity can last more than 20 min. Intercalibration of GEO sensors is considered in Roithmayr et al. (2014); however, the forthcoming discussion here is limited to intercalibration of instruments in low Earth orbit.

In this paper we restrict our attention to the reflected solar radiation spectrometer, and perform a quantitative examination of opportunities to intercalibrate other reflected solar radiation instruments placed aboard two particular sun-synchronous spacecraft. The first of these is the Joint Polar Satellite System (JPSS), which passes through its ascending node at 1330 local time (LT); the second spacecraft is the Meteorological Operation (MetOp), whose local time of ascending node is 2130 LT. The JPSS instruments of interest are VIIRS and CERES, whereas MetOp carries the AVHRR. Each of these instruments scans in the cross-track direction (perpendicular to the groundtrack of the host spacecraft), and

our analysis is tailored to such behavior. Simulations of orbital motion over 1-yr intervals have been conducted to quantify geographic position, duration, and viewing angles of the measurements, as well as motion required of a 2 degrees of freedom instrument gimbal. Estimates are provided for monthly and seasonal numbers of ISS measurement samples that can be used to intercalibrate the aforementioned instruments.

The remainder of the paper consists of five sections. In the first of these we describe the CLARREO reflected solar radiation spectrometer in some detail, provide a definition of intercalibration, and determine the number of samples required for intercalibrating instruments on JPSS and MetOp. The second and third sections contain, respectively, a description of simulations of orbital motion and a presentation of simulation results. Estimates of the number of samples that can be obtained from the ISS orbit are given in the fourth section, and conclusions are provided in the final section.

2. CLARREO reference intercalibration goals and methodology

To investigate whether it is possible to perform intercalibration of reflected solar radiation instruments with measurements obtained from the ISS, we must first determine the number of samples (averaged groups of measurements) required to characterize parameters of interest for those instruments. Before doing so, we describe the CLARREO reflected solar radiation spectrometer requirements and features, and provide a technical definition of intercalibration.

a. CLARREO RS hyperspectral imager

Intercalibration methodology is intimately related to CLARREO reflected solar (RS) mission requirements and instrument features. The basic concept of the RS spectrometer is the retrieval of an at-sensor reflectance over the spectral range from 320 to 2300 nm, with 4-nm continuous spectral sampling and 8-nm spectral resolution (full width at half maximum Gaussian bandpass for each spectral channel), with a 0.5-km ground-projected instantaneous field of view, and a 100-km swath width at nadir (NASA 2012). The continuous 4-nm spectral sampling is motivated by limiting the aliasing of spectral reflectance measurements. Measurements of radiance while viewing Earth's surface will be converted to a reflectance through ratios to solar measurements (Wielicki et al. 2013). The measurement of Earth's reflected radiance will vary by an order of magnitude because it is functionally dependent on solar zenith angle, wavelength, atmospheric gas absorption that changes with altitude and wavelength, and scene type that ranges from dark (clear-sky ocean) to bright (deep convective clouds). The RS instrument must be designed to account for these effects and to include a calibration approach that allows accurate retrieval of the reflectance in the middle of the visible part of the spectrum, traceable to SI standards at a level better than 0.3% ($k = 2$) (National Research Council 2007; Fox et al. 2011; BIPM 2008). (We use k instead of σ to establish a rigorous tie between the climate science and metrology research communities; in the case of a Gaussian distribution, $k = 1$ signifies the same confidence level as 1σ.) This accuracy is required to drive decadal climate change observational uncertainties to levels smaller than the internal natural variability of the climate system (Wielicki et al. 2013; Leroy et al. 2008; Fox et al. 2011). The driving instrument requirements for the RS sensor are summarized in Table 1, where the solar zenith angle θ_0 at a point on Earth's surface is defined as the angle between local zenith and the line of sight to the sun.

TABLE 1. Driving requirements for CLARREO RS instrument.

Parameter	Instrument requirement
Radiometric accuracy	0.3% ($k = 2$) in broadband reflectance
Spectral range	320–2300 nm
Spectral sampling	4 nm
Instantaneous field of view	0.5 km × 0.5 km
Nadir swath width	100 km
Signal-to-noise ratio	>33 (for mean 0.3 reflectance at $\theta_0 = 75°$)

The primary data product from the RS instrument is spectral reflectance. The current operational plan for the RS instrument is to determine the ratio of the output of the instrument while viewing an Earth scene to that of the instrument while viewing the sun. Taking into account the geometric differences between a radiance measurement (while viewing the Earth scene) and an irradiance measurement (the solar measurement) permits the retrieval of a directional-hemispheric reflectance. Thus, the RS sensor will function like a band-ratioing radiometer. The instrument, based on an Offner imaging spectrometer design to limit spectral smile on the focal plane, will operate as a hyperspectral push broom imaging spectrometer. Attached to the ISS with a 2 degrees of freedom gimbal, the instrument can match the line of sight of the other sensor being intercalibrated; this results in similar viewing angles for the two sets of measurements.

To observe both Earth's reflected radiance and solar irradiance, the sensor must be able to reduce the incident solar energy by approximately a factor of 50 000 so that the resulting signal is comparable to the Earth-viewing

TABLE 2. Summary of high-priority intercalibration tasks. Viewing zenith angle is denoted as θ and degree of linear polarization as p. Relative error contribution from reference intercalibration for corresponding time period, and required intercalibration sample number N.

Sensor	Parameter	Time scale	Variable	Error (%) ($k = 2$)	N
CERES	Offset	Monthly	Scan angle	0.9	2.5×10^3
	Gain	Monthly	Scan angle	0.9	2.5×10^3
	Degradation of optics	Seasonally	Scene type	0.5	30×10^3
	Nonlinearity	Annually	All data	0.3	150×10^3
VIIRS and AVHRR	Baseline offset	Monthly	p, scan angle	0.9	7.0×10^3
	Baseline gain	Monthly	p, scan angle	0.9	7.0×10^3
	Sensitivity to polarization	Seasonally	p, θ	0.5	1.2×10^6
	Nonlinearity	Annually	p, scan angle	0.3	0.5×10^6

energy. The attenuator approaches being evaluated include a single pinhole aperture, neutral density filters, a collection of pinhole apertures, or combinations of these three. The reason that three attenuator approaches are currently under study is that an additional goal of CLARREO calibration is to rely on multiple and independent calibration approaches. The attenuators require extremely careful evaluation during ground testing and are also a source of uncertainty on orbit if the attenuators degrade in some fashion. Evaluation of the attenuators on orbit takes place through coordinated views of the sun and the moon. The brightness of the moon is low enough to permit measurements without the attenuators in place, allowing coupled lunar and solar views to be used to determine if the attenuators are operating properly. Instrument nonlinearity is determined using a range of attenuators while observing the sun.

b. *CLARREO RS reference intercalibration approach*

We define reference intercalibration as multidimensional minimization of the difference between calibrated sensor measurements and CLARREO RS spectrometer high-accuracy SI-traceable measurements, performed for all available matched sampling. Intercalibrated instrument response parameters are relative to the CLARREO SI-traceable reference and derived over a time period (month, season, year). The intercalibration approach is based on retrieval of instrument offset and gain for every intercalibration data configuration, by comparison with CLARREO as a high-accuracy reference. It is essential that every intercalibration data configuration is provided with adequate sampling to reduce statistical data matching noise between CLARREO and intercalibrated sensor observations and to allow offset and gain retrieval with additional uncertainty, comparable to CLARREO instrument accuracy, 0.3% ($k = 2$) over a climate autocorrelation time period of 0.8 years (Wielicki et al. 2013, their Table 1). Thus, the combined intercalibration transfer uncertainty is limited to about $\sqrt{2} \times 0.3\%$ ($k = 2$). Additional uncertainty contributions to the intercalibration error budget can arise from spectral aliasing for imagers (e.g., VIIRS) and integration into broad band (e.g., CERES). The uncertainty due to CLARREO reflected solar spectrometer (RSS) spectral features is the subject of a separate study.

c. *CLARREO RS reference intercalibration objectives*

We prioritize CLARREO intercalibration tasks separately for CERES and for the VIIRS and AVHRR imagers. High-priority intercalibration tasks are summarized in Table 2 for these instruments, with an indication of required intercalibration time scale and variable for data stratification. The required limit on the intercalibration error contribution is based on the assumption that all monthly and seasonal calibrations are independent over a climate autocorrelation time period of 0.8 years. The number of intercalibration samples required to reduce the error to the stated value is denoted by N.

The highest priorities for CERES intercalibration are gain, scan-angle-dependent electronic offset, and correction of spectral response function (Clark and DiBattista 1978). CERES bolometer detectors are designed and verified to achieve less than 0.1% nonlinearity, and the spherical symmetry of the Cassegrain optics is designed to eliminate polarization sensitivity (Wielicki et al. 1996). The spectral response function is very broad (350–3500-nm wavelength), but optics contamination for all reflected solar sensors typically occurs below 500 nm; therefore, spectral response must be verified for achieving climate accuracy.

For CLARREO intercalibration of VIIRS and AVHRR, the highest priorities are the baseline offset, gain, nonlinearity, and gain corrections due to sensitivity to polarization. VIIRS sensitivity to polarization is reported to be up to 3%, depending on band, detector, and viewing

geometry (Fest 2009). Sensitivity to polarization is a response of the optical system, and it results in an additional contribution to effective gain, depending on scene type and viewing geometry. One important characterization of viewing geometry is the viewing zenith angle θ, which is defined at a point on Earth's surface to be the angle between local zenith and the line of sight to the orbiting instrument of interest. The strong angular dependence of Earth scene degree of polarization (Nadal and Bréon 1999) makes it necessary to change the direction in which the CLARREO RS sensor is aimed in order to intercalibrate imager sensitivity to polarization. This is accomplished by mounting the RS sensor on a 2 degrees of freedom gimbal, as discussed presently. Change in the imager optics response function, such as a central wavelength shift of narrow band, is reported to be small for both MODIS instruments on the *Terra* and *Aqua* platforms (Xiong et al. 2006b,a); therefore, its detection is not given a high priority.

Simulations of CLARREO intercalibration were carried out to establish the sensitivity of views matched in time, space, and angles, to the accuracy of the matching (Wielicki et al. 2008). These matching constraints were determined using data from 2 months of AVHRR *National Oceanic and Atmospheric Administration-17* (*NOAA-17*) and *NOAA-18* orbit crossings. Intercalibration data matching noise is limited to 1% by following recommendations in Wielicki et al. (2008). For spatial matching with CLARREO RSS observations, we require averaging over a 10 km × 10 km area for VIIRS intercalibration and spatial convolution over the point spread function (about 20 km in diameter at nadir) for CERES intercalibration. Angular matching (solar zenith, viewing azimuth, viewing zenith angles) is required to be within ±1.5°, and time matching is required to be within 5 min. Our sampling requirement for intercalibration noise reduction is based on this noise level.

To derive the number N (see Table 2) of required intercalibration data samples, we performed a set of additional simulations. We started with orbital modeling of CLARREO in LEO, pointing the CLARREO RS boresight to match the viewing geometry of the target sensor. Using the results from orbital modeling, and existing CERES and *Polarization and Anisotropy of Reflectances for Atmospheric Sciences Coupled with Observations from a Lidar* (*PARASOL*) data,[1] we estimated the expected scene type and polarization distributions over one year of CLARREO intercalibration operations. Then we simulated the intercalibration algorithms using existing Scanning Imaging Absorption Spectrometer for Atmospheric Cartography (SCIAMACHY) spectral data[2] as a proxy for CLARREO RS measurements, adding data matching noise statistically. Finally, combining inputs from all these steps and modeling the data-taking modes of the intercalibrated sensors, along with the CLARREO RS instrument spatial coverage, we estimated both the required and the achievable intercalibration sampling for the target sensors.

3. Description of orbital simulations

As discussed in Roithmayr and Speth (2012), analysis of opportunities for intercalibration over long periods is made computationally efficient by adopting several simplifying assumptions regarding orbital motions of two spacecraft about Earth, Earth's orbit about the sun, and Earth's shape. In short, all orbits are treated as circular, and Earth is considered to have a spherical surface. Precession of a spacecraft's orbit plane with respect to an inertial reference frame is taken into account by employing a well-known expression for orbital average nodal regression rate as a function of inclination of the orbit plane, radius of the orbit, and the parameter J_2 that quantifies Earth's oblate mass distribution. For convenience, each simulation begins at the instant of autumnal equinox.

Because measurements of reflected solar radiation are of interest, solar illumination of Earth's surface must be considered when determining whether an opportunity for intercalibration exists. For the purposes of the analysis discussed here, a necessary condition for intercalibration is that the subsatellite points of both spacecraft must lie on the illuminated hemisphere to include the terminator.

Provided the foregoing condition of illumination is satisfied, an intercalibration opportunity is regarded as the period of time during which ISS is inside a "tent" that is attached to the second spacecraft, say, JPSS, as illustrated in Fig. 1. The field of view of the JPSS instrument has an angular displacement to either side of nadir; this scan angle, taken here to be 55°, determines the slope of the roof of the tent. Reflected solar radiation lies in the shortwave region of the spectrum and the scenes observed by the instrument change rapidly; consequently, a limit is imposed on the time elapsed between

[1] We used the CERES Single Scanner Footprint (SSF) Edition 3 data product distributed by NASA, and the *PARASOL* level 1 data product distributed by Centre National d'Études Spatiales (CNES), France.

[2] We used the SCIAMACHY SCI_NL_ _1P data product distributed by the European Space Agency. We used version 7.03 of the data and the corresponding level 1C radiometric calibration tool, and version 7.01 of *m*-factor correction for instrument optics degradation.

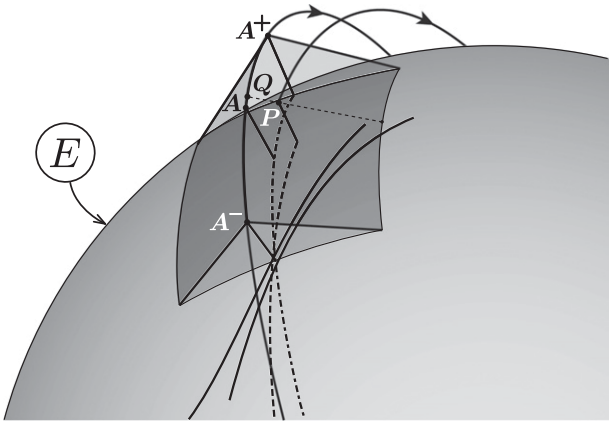


FIG. 1. Earth's surface is indicated by E. The black curves with arrows show the orbit tracks of ISS, P, and satellite, A, carrying the cross-track scanning instrument being calibrated. Point A^+ is 5 min ahead of A; A^- is 5 min behind A. Intercalibration opportunity is the period of time during which ISS is inside a tent that is attached to A. ISS instrument boresight is aimed along line QP. Within the boundaries of the ISS instrument swath, indicated by solid black curves on E, the reference intercalibration data will be closely matched to measurements of the sensor on A. When ISS exits the tent, the intercalibration opportunity ends.

measurements obtained by the two spacecraft (Wielicki et al. 2008). Analysis is performed in this study with a temporal constraint of 5 min. In Fig. 1, point A denotes the actual position of JPSS. The temporal constraint is imposed by imagining a spacecraft A^+ that is 5 min ahead of A in its orbit and another spacecraft A^- that is 5 min behind A. The arc that passes through A^+, A, and A^- forms the ridge of the tent's roof. When ISS, denoted by P, is inside the tent, an intercalibration opportunity exists. At any instant, one point Q on the ridge of the tent is closest to P. The ISS sensor is aimed toward Earth E, such that the boresight is parallel to the line joining Q and P; thus, at the resulting target on the surface of E, the viewing zenith angle to P (the angle θ between local zenith and the line of sight to P) is the same as the viewing zenith angle to Q. The boundaries of the ISS instrument swath are indicated with solid black curves. As measurement points in the instrument field of view move farther away from the boresight target, in a direction that is perpendicular to the JPSS groundtrack, the difference in viewing zenith angles to P and to Q becomes greater, and the measurement becomes less useful for the purpose of intercalibration.

Alignment of the ISS sensor boresight with the line of sight QP (see Fig. 1) is facilitated by attaching the instrument to the ISS with a gimbal that permits rotational motion about two orthogonal axes. Here, we use a particular configuration of gimbal axes, the first of which is parallel to the ISS z (or yaw) axis and the second of which is parallel to the instrument's x (or roll) axis. The angular displacements about the yaw and roll axes are denoted by q_1 and q_2, respectively. The yaw–roll gimbal sequence is attractive because the value of q_1 needed to aim the boresight also makes the ISS instrument swath parallel to the swath of the instrument being intercalibrated. Nominally, the ISS instrument scan plane is perpendicular to the ISS groundtrack when $q_1 = 0°$, whereas the scan plane is parallel to the groundtrack for $q_1 = 90°$. The effective swath width is, in the first instance (with $q_2 = 0°$), 100 km and, in the second case, 0.5 km. Measurements associated with a narrow effective swath are not useful for intercalibration. In this study the values of q_1 and q_2 are calculated under the assumption that the ISS x, y, and z axes are parallel to the axes of a local-vertical-local-horizontal reference frame. The ISS torque equilibrium attitude (TEA) differs from this idealization, but each of the three TEA angles is typically expected to be less than 15° and to vary slowly (Gomez 2010). The values of q_1 and q_2 reported here are therefore expected to be a good first approximation, and moderate adjustments to those values will enable the instrument gimbal to compensate for ISS attitude motion.

For the sake of simplicity, it is assumed in this paper that no part of the ISS structure obstructs the instrument field of view. Depending on the instrument mounting location, varying levels of partial view obstruction may at times occur (NASA 2007). With a particular site specified for the instrument, a corresponding reduction in measurements (and sampling numbers) can be determined.

Simulations of orbital motion during a 1-yr period have been performed to examine intercalibration opportunities between ISS and two other spacecraft, JPSS and MetOp, which are in near-polar, sun-synchronous orbits that pass through their respective ascending nodes at 1330 LT (afternoon) and 2130 LT (night). Orbital parameters for each spacecraft are presented in Table 3.

4. Orbital simulation results

In what follows, orbital simulation results are presented in several plots, accompanied by discussion. The plots illustrate the ISS groundtrack during each intercalibration opportunity, a time history of groundtrack latitude at the beginning of each opportunity, the ISS instrument swath during two particular opportunities, time histories of opportunity duration, envelopes of angles characterizing viewing geometry, and envelopes of gimbal angles, along with first and second time derivatives of the gimbal angles.

TABLE 3. Orbital parameters of ISS, JPSS, and MetOp.

Orbital parameter	ISS		JPSS (1330 LT)		MetOp (2130 LT)	
Altitude (km)	(constant)	400	(constant)	833	(constant)	817
Inclination, i (°)	(constant)	51.6	(constant)	98.74	(constant)	98.68
Right ascension, Ω (°)	($t = 0$)	0	($t = 0$)	202.5	($t = 0$)	322.5
Arg of latitude, υ (°)	($t = 0$)	0	($t = 0$)	0	($t = 0$)	0

Figure 2 shows the ISS groundtrack during each opportunity to take measurements for intercalibrating JPSS sensors. The number of opportunities in one year is determined to be 790. The groundtracks remain within 51.6° of the equator, but are otherwise well distributed in longitude as well as latitude, which is an indication that the measurements are also well distributed geographically. The length of the groundtrack is proportional to the duration of the opportunity. The number of opportunities over the year to intercalibrate MetOp is found to be 772; ISS groundtracks during these opportunities are displayed in Fig. 3.

The latitude of the ISS subsatellite point at the beginning of each opportunity for JPSS intercalibration is plotted over the course of one year in Fig. 4, where time $t = 0$ corresponds to the instant of autumnal equinox. The sinusoidal behavior has a 60-day period, which corresponds to the length of the cycle in nodal alignments for the ISS and a sun-synchronous orbit. A similar plot has been constructed for MetOp, but it is omitted in the interest of conciseness. As one would expect, the main difference in the two plots consists of a phase shift corresponding to the difference in local times of the nodal crossings of JPSS and MetOp.

Details of the ISS instrument swath during two intercalibration opportunities are provided in Fig. 5. Dashed–dotted curves indicate the ISS ground tracks; a diamond and a square mark the beginning and end of each opportunity, respectively. The boresight of the ISS instrument is directed along the track marked by solid circles; at every point on this curve, the line of sight to ISS is the same as it is to JPSS. The boundaries of the ISS instrument swath are shown with dashed curves. (When the ISS instrument is directed at nadir, the width of the swath is 100 km.) During some opportunities, the swaths extend as far as latitudes 52.18°N or 52.18°S.

The duration of each JPSS intercalibration opportunity is shown in Fig. 6, depending on whether solar zenith angle θ_0 is taken into account. According to Minnis et al. (2008), measurements of reflected solar radiation are useful for intercalibration only when $\theta_0 \leq 75°$. This constraint is left out of account in the top plot of Fig. 6, whereas the constraint is applied at the ISS instrument boresight target in determining the durations shown in the bottom plot. The constraint affects the duration at three times during the year, for only a few days each time, and reduces the total yearly duration from 1.41 to 1.36 days. The 60-day nodal alignment cycle is evident in these results. The opportunities having the longest durations, nearly 300 s, occur over near-equatorial latitudes as both spacecraft are ascending or descending together through the equatorial plane. Secondary maxima of

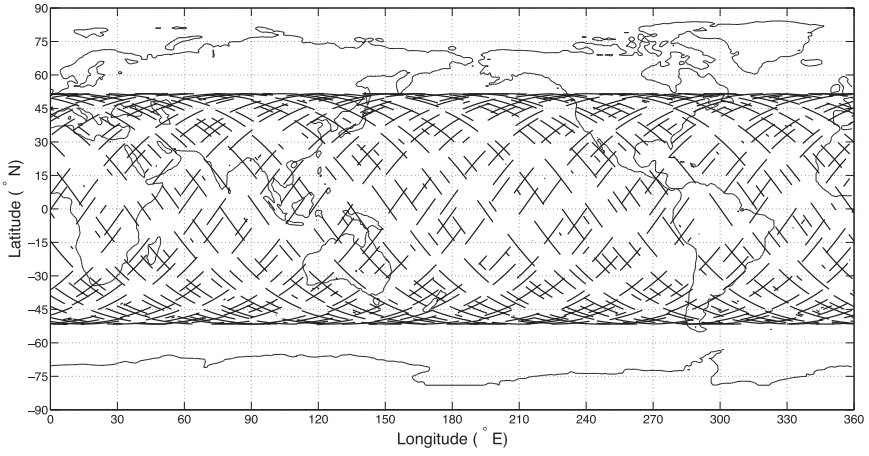


FIG. 2. A 1-yr distribution of 790 intercalibration opportunities, ISS vs JPSS.

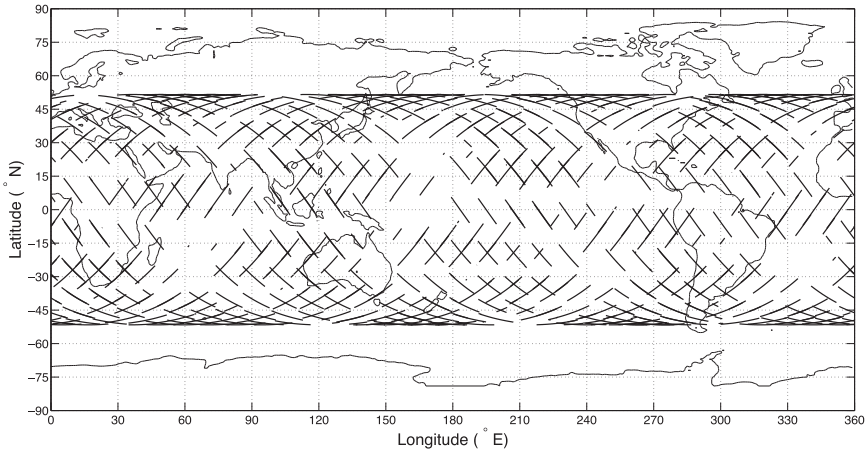


FIG. 3. A 1-yr distribution of 772 intercalibration opportunities, ISS vs MetOp.

approximately 240 s occur at times when one spacecraft is ascending and the other is descending through the equatorial plane. The minima with values of around 180 s correspond to opportunities taking place over high latitudes, where the angle between the two orbit planes is greatest.

Durations of opportunities to intercalibrate MetOp sensors are plotted in Fig. 7. In the case of MetOp, the total yearly opportunity duration is 1.34 days in the absence of a solar zenith angle constraint, whereas it decreases to 1.23 days when the constraint is applied.

Three viewing angles are important in connection with measuring solar radiation reflected from a point T on Earth's surface. Two of the angles have already been introduced: the viewing zenith angle θ and the solar zenith angle θ_0. The third angle, referred to as the relative azimuth angle ϕ is measured between two planes that intersect on the local zenith line: one of the planes contains the line of sight from T to a spacecraft and the other plane contains the line of sight from T to the sun. Values of ϕ range from 0° to 360°.

Maximum and minimum values of all three viewing angles at the ISS instrument boresight target are plotted in Fig. 8 for each JPSS intercalibration opportunity over a year. The upper bound on the viewing zenith angle is about 68°. The solar zenith angle has a global maximum of approximately 85°, and exceeds 75° on three occasions for several days each. It is during these three intervals that the useful durations drop noticeably in the bottom plot of Fig. 6. For the first 30 days or so, the relative azimuth angle ranges roughly between 120° and 300°. Over the next 30-day period, the bounds are approximately 60° and 240°. This pattern repeats itself thereafter. A 180° difference between maximum and minimum is

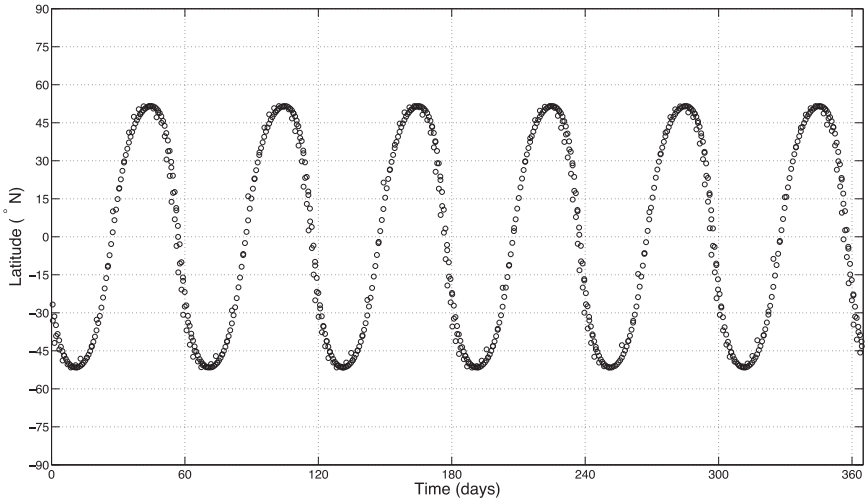


FIG. 4. ISS latitude at the start of each opportunity, JPSS.

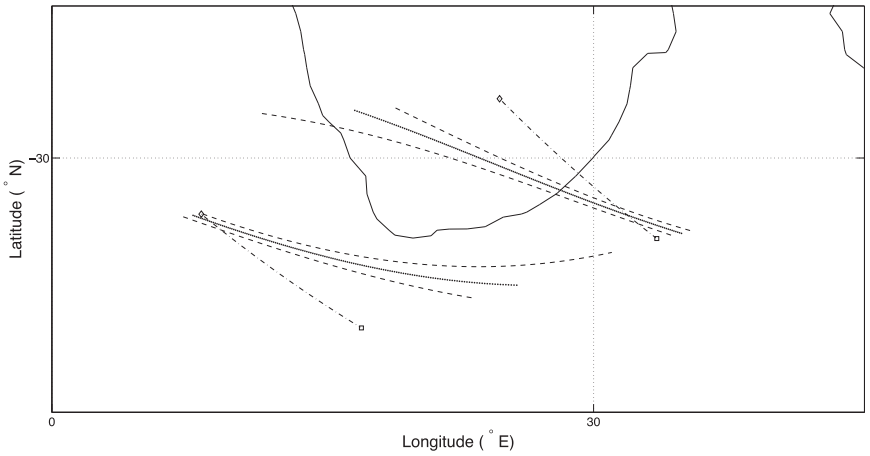


FIG. 5. ISS instrument swaths for two intercalibration opportunities, JPSS: ISS groundtrack (dashed–dotted), ISS instrument boresight (solid circles), and swath boundaries (dash).

indicative of a discontinuity in relative azimuth angle as ISS passes under the ridge of the tent (see Fig. 1) during a typical opportunity. Plots of viewing angle extrema for MetOp intercalibration opportunities are similar to those in Fig. 8 and are omitted in the interest of brevity.

During each JPSS intercalibration opportunity, the ISS instrument gimbal must move such that the boresight remains parallel to the line of sight from JPSS to ISS. Behavior of the yaw gimbal is illustrated in Fig. 9 where, for each opportunity, the maximum and minimum gimbal angle q_1, angular speed $\dot{q}_1$, and angular acceleration $\ddot{q}_1$ are shown in the top, middle, and bottom plots, respectively. The 60-day nodal alignment cycle is once again apparent. The yaw gimbal is not required to move much during each opportunity, as can be seen by inspecting the plots for q_1 and $\dot{q}_1$. The gimbal angular speed need not exceed $0.006°\,s^{-1}$ in absolute value. On the other hand, Fig. 10 shows the roll gimbal will need to be more active than the yaw gimbal. Excursions in q_2 during each opportunity will typically be about 110°, which is twice the value of the scan angle of the instruments on JPSS. The roll gimbal will be required to produce an angular speed $\dot{q}_2$ of around $1.1°\,s^{-1}$ in absolute value. The plot of $\ddot{q}_2$ indicates a maximum of about $0.013°\,s^{-2}$ is needed. Torque motors for the yaw and roll gimbals can be sized according to the global maximum values of $\ddot{q}_1$ and $\ddot{q}_2$ obtained from Figs. 9 and 10, respectively.

As mentioned previously, some adjustments to Figs. 9 and 10 are necessary to account for ISS TEA motion.

The envelopes of $\dot{q}_i$ and $\ddot{q}_i$ $(i = 1, 2)$ presented in Figs. 9 and 10 lie inside those associated with a nominal

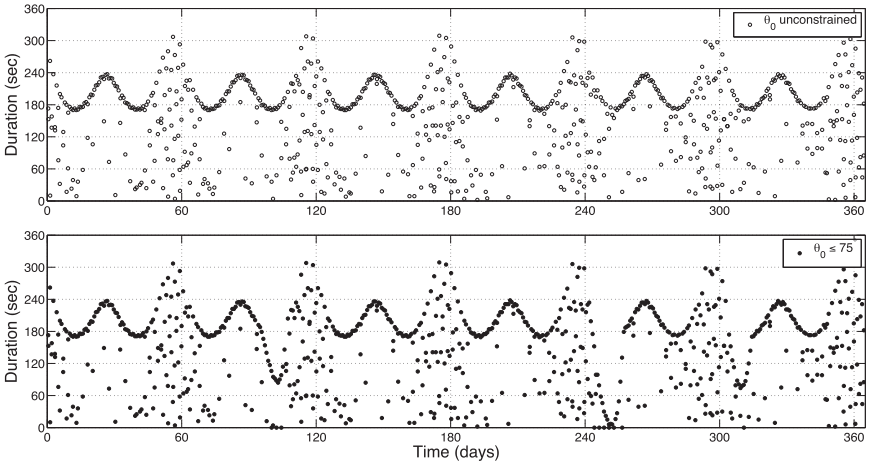


FIG. 6. Durations of intercalibration opportunities, ISS vs JPSS.

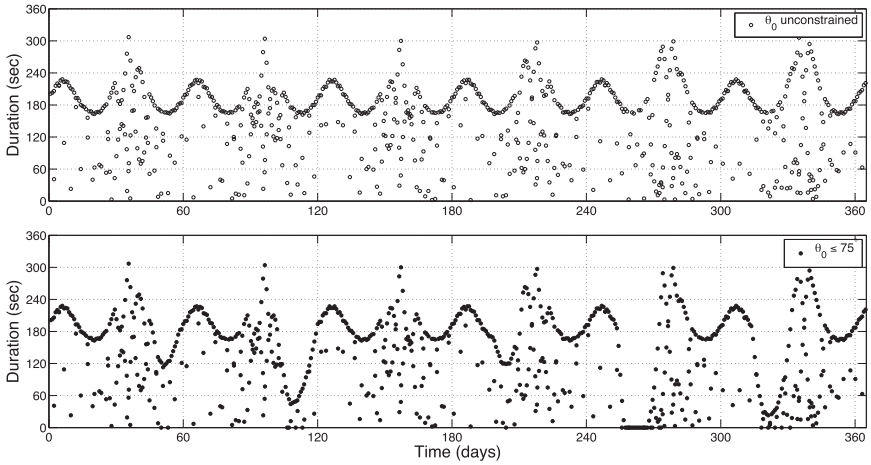


FIG. 7. Durations of intercalibration opportunities, ISS vs MetOp.

CLARREO orbit (altitude 609 km, inclination 90°). The difference in orbital altitudes of CLARREO and JPSS was approximately 200 km, whereas the altitudes of ISS and JPSS differ by about 400 km; the line of sight between spacecraft changes direction more gradually in the latter pairing.

5. Reference intercalibration sampling

Here, we construct intercalibration samples for the VIIRS and AVHRR instruments such that spatial matching noise is limited to 1%, with data constraints described in section 2. This is accomplished by defining a sample in angular space as 1.5° of elevation angle of the instrument, which corresponds from the ISS orbit to a nadir equivalent area of 10 km × 10 km. Two samples having independent spatial noise are related to each other by a shift of 0.15° in elevation angle, which results in a 1-km shift in each of two spatial directions, along and perpendicular to the groundtrack. The CLARREO spatial resolution of 0.5 km × 0.5 km ensures the two samples have only two boundary pixels in common. We estimate the number of samples by shifting them in this way. (It should be noted that this approach to forming samples does not allow intercalibration on a detector-by-detector basis; relative calibration of VIIRS detectors to each other requires use of VIIRS data alone—the same is true of AVHRR detectors.)

The number of CLARREO samples that can be used to intercalibrate CERES is estimated by taking into account the size of the CERES point spread function at 2.6° in the along-track direction, and a data acquisition rate of 330 measurements in each 180° cross-track scan performed over 3.3 s (Wielicki et al. 1996).

Using the orbital simulation results presented in the previous section, we estimate the projected number of

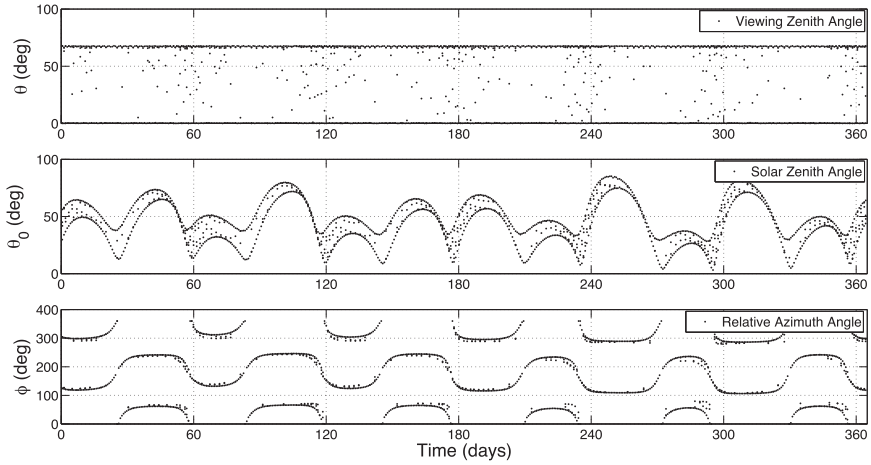


FIG. 8. Viewing angles at boresight target: min and max values in each opportunity, ISS vs JPSS.

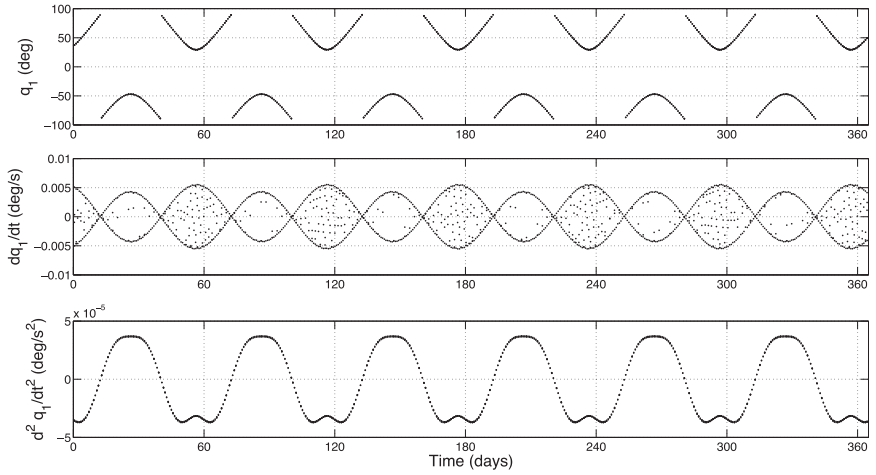


FIG. 9. Yaw gimbal motion: min and max values in each opportunity, ISS vs JPSS.

intercalibration samples for VIIRS and CERES instruments on the JPSS, and the AVHRR instrument on the MetOp satellite. All estimates are made with the following constraints: (i) $\theta_0 < 75°$ (to ensure high signal-to-noise ratio); (ii) CLARREO effective swath width is greater than 10 km for VIIRS and AVHRR, and greater than 25 km for CERES; (iii) θ is matched within 1.5°, θ_0 and ϕ are matched within 1°; and (iv) intercalibration event duration is greater than 10 s. The sampling estimates are presented in Fig. 11, reported by month in the top plot, and by season in the bottom plot. Comparison of these estimates with Table 2 shows that the number of samples is sufficient to intercalibrate well-behaved sensors in JPSS and MetOp orbits within the uncertainty required for measuring long-term climate change. Over a climate autocorrelation time period of 0.8 years, the statistical uncertainty contribution from data matching can be contained within 0.3% ($k = 2$).

6. Conclusions

The International Space Station is ideally suited to serve as a platform from which to obtain reflected solar radiance measurements that can be used to intercalibrate instruments in sun-synchronous low Earth orbits. The ISS orbit provides coverage of a large part of the globe, which extends from 52.18°S to 52.18°N latitude. All scene types necessary for intercalibration, including clouds, snow, clear-sky ocean, desert, and vegetation, can be found within the area of coverage. Results of orbital simulations show that the difference in ISS and sun-synchronous orbit plane precession leads to temporal uniformity in opportunities for intercalibration. Angular speed and angular acceleration required from a 2 degrees of freedom instrument gimbal for matching line of sight on ISS compares favorably to what is required for a dedicated CLARREO mission.

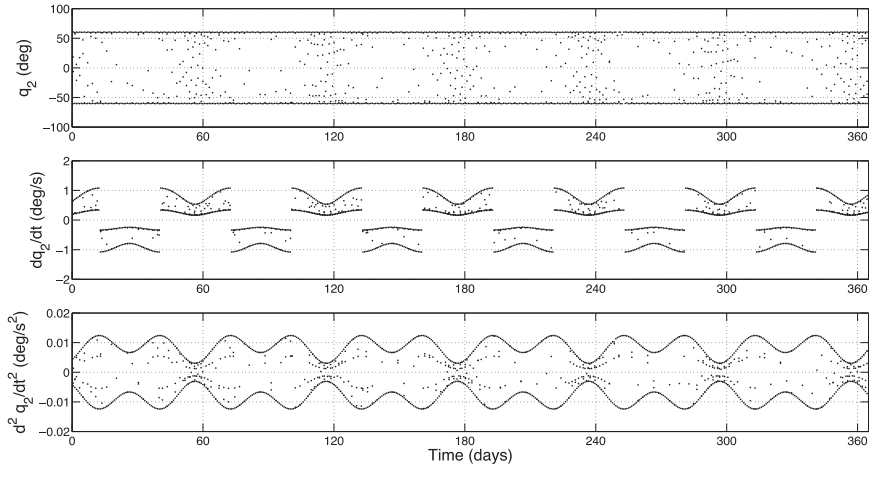


FIG. 10. Roll gimbal motion: min and max values in each opportunity, ISS vs JPSS.

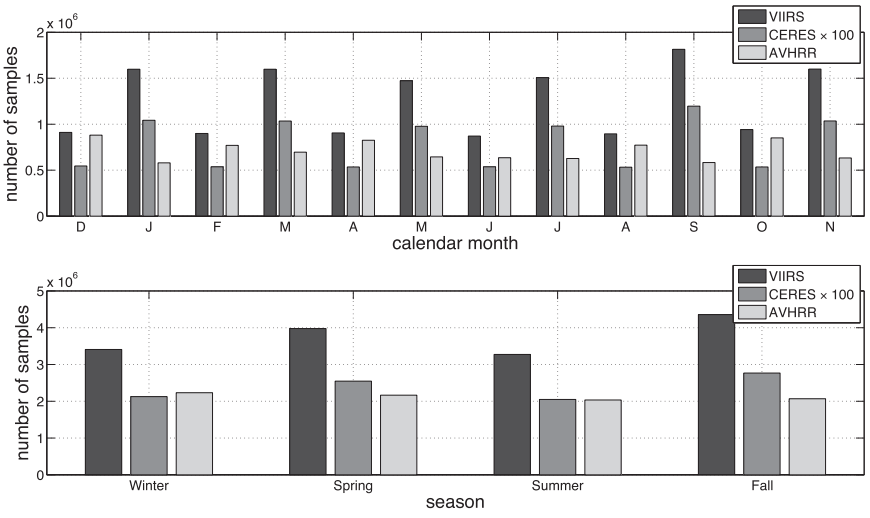


FIG. 11. Monthly and seasonal sampling estimates, ISS vs the following: JPSS-VIIRS, JPSS-CERES, and MetOp-AVHRR.

The number of samples that can be obtained from ISS is sufficient to intercalibrate well-behaved sensors in sun-synchronous low Earth orbits to the accuracy required for measuring long-term climate change. With restrictive data matching, the intercalibration statistical uncertainty can be limited to 0.3% ($k = 2$) over a climate autocorrelation time period of 0.8 years. Using a CLARREO reflected solar sensor as a high-accuracy orbiting standard for comprehensive reference intercalibration of other instruments would improve their accuracy substantially, and thereby add significant value to the existing Earth Observing System.

REFERENCES

BIPM, 2008: Evaluation of measurement data—Guide to the expression of uncertainty in measurement. Joint Committee for Guides in Metrology, Bureau International des Poids et Mesures, 120 pp. [Available online at http://www.bipm.org/utils/common/documents/jcgm/JCGM_100_2008_E.pdf.]

Clark, L. G., and J. D. DiBattista, 1978: Space qualification of optical instruments using the NASA Long Duration Exposure Facility. *Opt. Eng.,* **17,** 175547, doi:10.1117/12.7972276.

ESA, 2011: Research announcement for International Space Station experiments relevant to study of global climate change. European Space Agency, Directorate of Human Spaceflight and Operations, Directorate of Earth Observation Programmes, Noordwijk, Netherlands, 22 pp. [Available online at http://wsn.spaceflight.esa.int/docs/201107/ESA-ISS-Climate-Change-Experiments-Research-Announcement.pdf.]

Fest, E. C., 2009: VIIRS polarization sensitivity testing and analysis. *Polarization Science and Remote Sensing IV,* J. A. Shaw and J. Scott Tyo, Eds., International Society for Optical Engineering (SPIE Proceedings, Vol. 7461), 746102, doi:10.1117/12.828154.

Fox, N. P., and Coauthors, 2003: Traceable radiometry underpinning terrestrial- and helio-studies (TRUTHS). *Sensors, Systems, and Next-Generation Satellites VI,* H. Fujisada et al., Eds., International Society for Optical Engineering (SPIE Proceedings, Vol. 4881), 395–406, doi:10.1117/12.462438.

——, A. Kaiser-Weiss, W. Schmutz, K. Thome, D. Young, B. Wielicki, R. Winkler, and E. Woolliams, 2011: Accurate radiometry from space: An essential tool for climate studies. *Philos. Trans. Roy. Soc. London,* **A369,** 4028–4063, doi:10.1098/rsta.2011.0246.

Goldberg, M., and Coauthors, 2011: The Global Space-Based Inter-Calibration System. *Bull. Amer. Meteor. Soc.,* **92,** 467–475, doi:10.1175/2010BAMS2967.1.

Gomez, S., 2010: GNC performance requirements and predicted performance estimates. Memo. EG-DIV-10-040, NASA, Johnson Space Center, 2 pp.

Leroy, S. S., J. G. Anderson, and G. Ohring, 2008: Climate signal detection times and constraints on climate benchmark accuracy requirements. *J. Climate,* **21,** 841–846, doi:10.1175/2007JCLI1946.1.

Minnis, P., D. R. Doelling, L. Nguyen, W. F. Miller, and V. Chakrapani, 2008: Assessment of the visible channel calibrations of the VIRS on TRMM and MODIS on *Aqua* and *Terra*. *J. Atmos. Oceanic Technol.,* **25,** 385–400, doi:10.1175/2007JTECHA1021.1.

Nadal, F., and F.-M. Bréon, 1999: Parameterization of surface polarized reflectance derived from POLDER spaceborne measurements. *IEEE Trans. Geosci. Remote Sens.,* **37,** 1709–1718, doi:10.1109/36.763292.

NASA, 2007: Overview of attached payload accommodations and environments on the International Space Station. NASA Tech. Publ. TP-2007-214768, 40 pp. [Available online at http://www.nasa.gov/pdf/190373main_TP-2007-214768.pdf.]

——, cited 2011: Announcement of Opportunity for the Earth System Science Pathfinder Program: Earth Venture-2. Science Mission Directorate, Solicitation NNH11ZDA012O. [Available online at https://www.fbo.gov/spg/NASA/HQ/OPHQDC/NNH11ZDA012O/listing.html.]

——, 2012: 2012 annual report. National Aeronautics and Space Administration, Earth Science Technology Office, 16 pp. [Available online at http://esto.nasa.gov/files/AnnualReports/2012ESTOAnnualReport.pdf.]

National Research Council, 2007: *Earth Science and Applications from Space: National Imperatives for the Next Decade and Beyond.* National Academies Press, 456 pp.

Roithmayr, C. M., and P. W. Speth, 2012: Analysis of opportunities for intercalibration between two spacecraft. *Advances in Engineering Research,* V. M. Petrova, Ed., Vol. 1, Nova Science Publishers, 409–436.

——, C. Lukashin, P. W. Speth, G. Kopp, K. J. Thome, B. A. Wielicki, and D. F. Young, 2014: CLARREO approach for reference intercalibration of reflected solar sensors: On-orbit data matching and sampling. *IEEE Trans. Geosci. Remote Sens.,* **52,** doi:10.1109/TGRS.2014.2302397.

Wielicki, B. A., B. R. Barkstrom, E. F. Harrison, R. B. Lee, G. L. Smith, and J. E. Cooper, 1996: Clouds and the Earth's Radiant Energy System (CERES): An Earth Observing System experiment. *Bull. Amer. Meteor. Soc.,* **77,** 853–868, doi:10.1175/1520-0477(1996)077<0853:CATERE>2.0.CO;2.

——, D. R. Doelling, D. F. Young, N. G. Loeb, D. P. Garber, and D. G. MacDonnell, 2008: Climate quality broadband and narrowband solar reflected radiance calibration between sensors in orbit. *2008 IEEE International Geoscience and Remote Sensing Symposium: Proceedings,* Vol. 1, IEEE, I-257–I-260, doi:10.1109/IGARSS.2008.4778842.

——, and Coauthors, 2013: Achieving climate change absolute accuracy in orbit. *Bull. Amer. Meteor. Soc.,* **94,** 1519–1539, doi:10.1175/BAMS-D-12-00149.1.

Xiong, X., N. Che, and W. L. Barnes, 2006a: Terra MODIS on-orbit spectral characterization and performance. *IEEE Trans. Geosci. Remote Sens.,* **44,** 2198–2206, doi:10.1109/TGRS.2006.872083.

——, ——, C. Pan, X. Xie, J. Sun, W. L. Barnes, and B. Guenther, 2006b: Results and lessons from MODIS reflective solar bands calibration: Pre-launch to on-orbit. *Earth Observing Systems XI,* J. J. Butler, Ed., International Society for Optical Engineering (SPIE Proceedings, Vol. 6296), 629607, doi:10.1117/12.679144.